Exploration of water jet generated by Q-switched laser induced water breakdown with different depths beneath a flat free surface

Ross C. C. Chen, Y. T. Yu, K. W. Su, J. F. Chen, and Y. F. Chen*

Department of Electrophysics, National Chiao Tung University, Hsinchu, Taiwan
*yfchen@cc.nctu.edu.tw

Abstract: The dynamics of a water jet on a flat free surface are investigated using a nanosecond pulsed laser for creating an oscillating bubble with different depths beneath the free surface. A thin jet is shown to deform a crater surface resulted from surface depression and cause a circular ring-shaped crater on the connection surface between the crater of surface depression and the thin jet. The collapse of this circular ring-shaped crater is proposed to the crown-like formation around a thick jet. The evolution of the bubble depth suggests a classification of four distinctive ranges of the bubble depths: non-crown formation when the parameter of bubble depth over the maximum bubble radius $\gamma \leq 0.5$, unstable crown formation when $0.5 \leq \gamma \leq 0.6$, crown-like structure with a complete crown wall when $0.6 \leq \gamma \leq 1.1$, and non-crown formation when $1.1 \leq \gamma$. Furthermore, the orientation of the crown wall gradually turns counterclockwise to vertical direction with increasing γ from 0.5 to 1.1, implying a high correlation between the orientation of the crown wall and the depth of the bubble. This correlation is explained and discussed by the directional change of the jet eruption from the collapse of circular ring-shaped crater.

OCIS codes: (140.3440) Laser-induced breakdown; (350.3390) Laser materials processing; (170.6920) Time-resolved imaging.

References and links

1. R. H. Cole, *Underwater Explosions* (Princeton, Princeton Univ. Press., 1948).
2. J. B. Keller and I. I. Kolodner, "Damping of underwater explosion bubble oscillations," J. Appl. Phys. **27**(10), 1152–1161 (1956).
3. A. Pearson, E. Cox, J. R. Blake, and S. R. Otto, "Bubble interactions near a free surface," Eng. Anal. Bound. Elem. **28**(4), 295–313 (2004).
4. G. L. Chahine, "Interaction between an oscillating bubble and a free Surface," J. Fluids Eng. **99**(4), 709–716 (1977).
5. P. B. Robinson, J. R. Blake, T. Kodama, A. Shima, and Y. Tomita, "Interaction of cavitation bubbles with a free surface," J. Appl. Phys. **89**(12), 8225–8237 (2001).
6. R. H. Mellen, "An experimental study of the collapse of a spherical Cavity in Water," J. Acoust. Soc. Am. **28**(3), 447–454 (1956).
7. A. Pain, B. H. T. Goh, E. Klaseboer, S. W. Ohl, and B. C. Khoo, "Jets in quiescent bubbles caused by a nearby oscillating bubble," J. Appl. Phys. **111**(5), 054912 (2012).
8. W. Lauterborn and H. Bolle, "Experimental investigations of cavitation-bubble collapse in the neighbourhood of a solid boundary," J. Fluid Mech. **72**(02), 391–393 (1975).
9. P. A. Quinto-Su, V. Venugopalan, and C. D. Ohl, "Generation of laser-induced cavitation bubbles with a digital hologram," Opt. Express **16**(23), 18964–18969 (2008).
10. J. C. Ramirez-San-Juan, E. Rodriguez-Aboytes, A. E. Martinez-Canton, O. Baldovino-Pantaleon, A. Robledo-Martinez, N. Korneev, and R. Ramos-Garcia, "Time-resolved analysis of cavitation induced by CW lasers in absorbing liquids," Opt. Express **18**(9), 8735–8742 (2010).
11. Y. Tomita, P. B. Robinson, R. P. Tong, and J. R. Blake, "Growth and collapse of cavitation bubbles near a curved rigid boundary," J. Fluid Mech. **446**, 259–283 (2002).
12. P. Gregorčič, R. Petkovšek, and J. Možina, "Investigation of a cavitation bubble between a rigid boundary and a free surface," J. Appl. Phys. **102**(9), 094904 (2007).

#179203 - $15.00 USD Received 2 Nov 2012; revised 19 Dec 2012; accepted 19 Dec 2012; published 4 Jan 2013

13. A. Philipp and W. Lauterborn, "Cavitation erosion by single laser-produced bubbles," J. Fluid Mech. **361**, 75–116 (1998).
14. R. Dijkink and C. D. Ohl, "Laser-induced cavitation based micropump," Lab Chip **8**(10), 1676–1681 (2008).
15. Y. Tomita and T. Kodama, "Interaction of laser-induced cavitation bubbles with composite surfaces," J. Appl. Phys. **94**(5), 2809–2816 (2003).
16. T. H. Wu, S. Kalim, C. Callahan, M. A. Teitell, and P. Y. Chiou, "Image patterned molecular delivery into live cells using gold particle coated substrates," Opt. Express **18**(2), 938–946 (2010).
17. M. Duocastella, A. Patrascioiu, J. M. Fernández-Pradas, J. L. Morenza, and P. Serra, "Film-free laser forward printing of transparent and weakly absorbing liquids," Opt. Express **18**(21), 21815–21825 (2010).
18. E. Klaseboer, B. C. Khoo, and K. C. Hung, "Dynamics of an oscillating bubble near a floating structure," J. Fluids Structures **21**(4), 395–412 (2005).
19. J. Li and J. Rong, "Bubble and free surface dynamics in shallow underwater explosion," Ocean Eng. **38**(17-18), 1861–1868 (2011).
20. B. R. Ringeisen, B. J. Spargo, and P. K. Wu, *Cell and Organ Printing* (Springer, 2010).
21. B. W. Zeff, B. Kleber, J. Fineberg, and D. P. Lathrop, "Singularity dynamics in curvature collapse and jet eruption on a fluid surface," Nature **403**(6768), 401–404 (2000).
22. A. M. Worthington and R. S. Cole, "Impact with a liquid surface, studied by the aid of instantaneous photography," Phil. Trans. Roy. Soc. **189**, 137–148 (1897).
23. S. T. Thoroddsen and A. Q. Shen, "Granular jets," Phys. Fluids **13**(1), 4–6 (2001).
24. J. M. Boulton-Stone and J. R. Blake, "Gas Bubble bursting at a free surface," J. Fluid Mech. **254**(-1), 437–466 (1993).
25. I. Apitz and A. Vogel, "Material ejection in nanosecond Er:YAG laser ablation of water, liver, and skin," Appl. Phys., A Mater. Sci. Process. **81**(2), 329–338 (2005).
26. S. T. Thoroddsen, K. Takehara, T. G. Etoh, and C. D. Ohl, "Spray and microjets produced by focusing a laser pulse into a hemispherical drop," Phys. Fluids **21**(11), 112101 (2009).

1. Introduction

Interaction between a bubble and a free surface is one of the most interesting topics in the field of bubble dynamics and has been studied extensively since the Second World War. These studies, dealing with a large-size explosion bubble in underwater explosion, mainly focused on the bubble oscillation and the generation of spray on the free surface [1,2]. Recently, a small-scale cavitation bubble in millimeter size was used and the results showed more qualitative behaviors compared to the large-size explosion bubble for further theoretical simulations [3]. Understanding these behaviors is believed to shed light on the mechanisms of the erosion damages on a deformable surface caused by a nearby collapsing bubble [4,5]. Such a small-scale bubble was generally generated by using spark discharge [6] and these studies showed that, universally, an oscillating bubble develops into a toroidal shape during its collapse [3–5]. This shape evolution was reconstructed well in theoretical simulations [3–5]. In addition to the bubble, a liquid jet was seen to burst out from the free surface, and for a certain bubble depth, there emerged a thin jet followed by a markedly thicker jet and a circular crown-like jet perfectly connected on the shoulder of the thick jet transited to the thin jet [4,7].

The main drawback of the spark discharge is the unavoidable influence of the electrodes on the dynamics of the bubble and liquid jet. In contrast, lasers have been shown to be useful and precisely controllable for generating a bubble by direct optical breakdown with pulsed lasers [8,9] or thermocavitation with CW lasers [10]. Several dynamics with different boundary systems was observed such as rigid wall for applications of erosion damages and fluid pumping [8,11–14], membrane or living cell for tissue engineering applications [15,16]. The oscillation times of a cavitation bubble near a rigid wall and free surface were investigated and compared with modified Rayleigh's model [12]. Very recently, a liquid jet on a flat free surface induced by a femtosecond pulsed laser was implemented in a new laser printing technique named film-free laser induced forward transfer (LIFT) to overcome the constraint of solid or liquid film preparation [17]. However, a liquid jet on a flat free surface by using a nanosecond pulsed laser with milli-joule energy has not yet been observed. Characterizing detailed morphology of a liquid jet for using such a pulse laser is important because it can be useful in large transfer applications such as pumping. Additionally,

#179203 - $15.00 USD Received 2 Nov 2012; revised 19 Dec 2012; accepted 19 Dec 2012; published 4 Jan 2013

compared to film-free LIFT, its more qualitative characteristics as will be shown can help understand on the forward transfer and the experimental results of spark discharge.

The most significant parameter affecting the dynamical properties of the liquid jet is the parameter γ of initial bubble depth over maximum bubble radius [3–5,11–15,18,19]. This γ is also a feasible technological parameter in several applications such as quality optimization in film-free LIFT [20, p.101]. Therefore, in this article, we characterize the liquid jet as a function of γ and investigate its morphology and generation. Experimentally, a nanosecond pulsed laser with wavelength 1064 nm is used to induce water breakdown, and a bubble with millimeter size is generated beneath a flat free surface. The overall behavior of interaction between the bubble and the free surface is recorded by a high speed camera. The liquid jet on the free surface can be divided into three parts, thin jet, thick jet, and crown-like structure around the thick jet, similar to the results of spark generations [4,7]. We find that the thin jet on the center of surface depression is crucial for crown formation and different morphologies of the crown-like structure appear with altering the bubble depth. A high regularity and correlation between the orientation of the crown wall and the bubble depth suggest that the crown-like formation is correlated to the surface depression with the thin jet.

2. Experiment

A schematic diagram of the experimental arrangement is shown in Fig. 1. A bubble is generated beneath the free surface by focusing a flash-pump pulsed laser (Nd:YAG, λ = 1064 nm) with a pulse width 6 ns from below a water tank vertically into tap water at a room temperature 297*K* under atmospheric pressure. The dimension of the tank is $100^{\backslash}70^{\backslash}20$ mm^3 and the depth of water is 13 mm for alleviating the influence on the bubble from the bottom wall of the tank. The output beam of the laser with beam waist 1.5 mm is enlarged 10 times its original size by employing a lens array with one biconcave lens and two convex lenses. Then, a lens with a focal length of 12 cm in air and a mirror with high-reflection coated at 1064 nm are used to focus the enlarged beam vertically beneath the free surface to form a point plasma followed by a cavitation bubble. The energy of the laser beam after the mirror is around 16 mJ and the maximum radius of the bubble is about 1.25 mm. The dynamic of the interaction between the bubble and the free surface is recorded by a high speed camera (NAC GX-3) which has maximum frame rate at 198,000 fps. The exposure time is automatically controlled by the high speed camera.

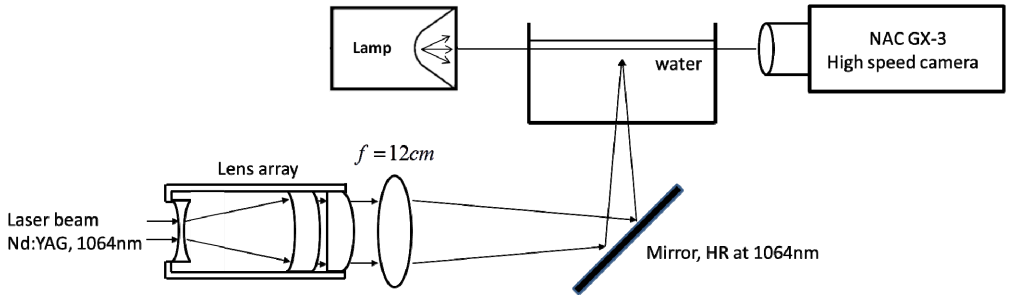

Fig. 1. Schematic diagram of the experimental setup.

3. Results and discussion

Figure 2 clearly shows the overall dynamic of a shallow underwater oscillating bubble and a water jet with complete structure and morphology on the free surface. The depth of the bubble from the free surface is 0.8 defined in stand-off parameter γ (h / R_{max}, h is initial distance between the center of the bubble and the free surface, R_{max} is maximum bubble radius). As shown, the bubble extrudes a thin jet during its period of first expansion, as similar as described in recent works [3–5], and the thin jet continues to rise after the first expansion. At

#179203 - $15.00 USD Received 2 Nov 2012; revised 19 Dec 2012; accepted 19 Dec 2012; published 4 Jan 2013

the end of the first expansion, the bubble starts to collapse due to the pressure decrease inside the bubble and moves downward, leading to the sinking around the surface on the bottom of the thin jet. This sinking surface was previously referred as surface depression [17]. When the sinking surface reaches its maximum depth, the surrounding water will flow toward the crater of the sinking surface, resulting in moving upward of the maximum depth point and the formation of the thick jet under the thin jet on the free surface [17]. Eruption of liquid jets from collapsing depressions has been observed in other circumstances, like standing Faraday-waves [21] and free-fall of a drop [22] on a liquid surface, and granular jets [23].

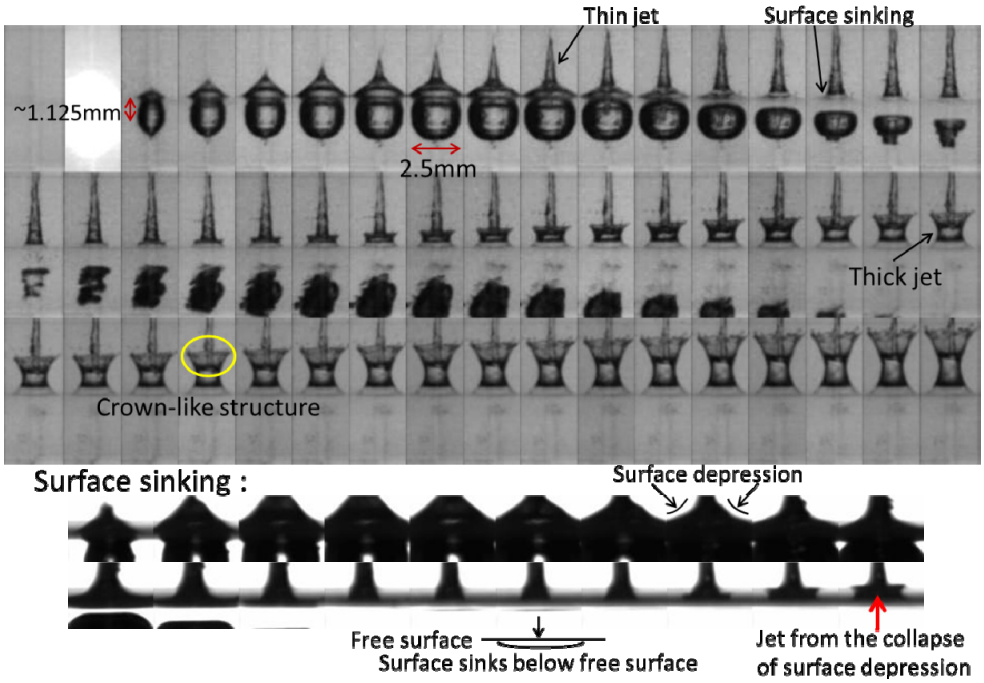

Fig. 2. A complete water jet is generated on a flat free surface with γ = 0.8. The frame rate is 80,000 fps. In the pictures of surface sinking, the exposure time is set to 1μs.

In the study of the free surface dynamics of shallow underwater explosion, the water jet on the free surface induced by TNT detonation shows a similar crown-like off-axis splash in theoretical simulation [18] and experimental observation [19], and the ring shaped prominence of the off-axis splash is extruded by the expanding boundary of the bubble. However, this expanding boundary cannot explain the formation of the crown-like structure in our observed results because the toroidal bubble collapses and rebounds downward away from the free surface, as shown in Fig. 2. In our observations, the complete crown wall is very smoothly connected to the surface of the thick jet, forming a perfect waist on the thick jet. Thus, there must be some correlations between the generation of the crown-like structure and the thick jet.

It should be noted that, before the formation of the thick jet, the thin jet has already formed on the sinking surface. This is in contrast to the general cases of surface depression in which only a crater (without the thin jet) appears on the free surface by inserting an external force [21–23] or a burst cavity just below the surface [24]. To help see the detailed surface curvature of the surface depression with a thin jet, we have applied the boundary integral method assuming a pressure $p = p_c + p_0(V_0/V)^{1.4}$ for a bubble in an inviscid, incompressible, and irrotational fluid domain, where p_c is a constant vapor pressure, V is the volume of bubble, and 1.4 the ratio of specific heats. Detailed numerical procedures of boundary integral

#179203 - $15.00 USD Received 2 Nov 2012; revised 19 Dec 2012; accepted 19 Dec 2012; published 4 Jan 2013

method can be obtained from Refs. 3,5. Figure 3 shows the simulated dynamics of the bubble and free surface, along with the detailed schematic curvature of the surface depression with the thin jet. In fluid systems, a surface depression usually causes a singularity or near singularity of certain physical observables such as the divergences of velocity, surface curvatures, or pressure gradients at the minimum depth or pinch-off point [21]. The collapse of a surface singularity or near singularity leads to a jet formation. As shown in Fig. 3, the cross-sectional schematic image shows three singularities or near singularities as denoted by three solid dots. The central dot, obtained by linearly extrapolating the symmetric curves of the free surface without the thin jet, results in a thick jet as previously observed in collapsing depression [17]. The surface connected from the crater to the thin jet contributes to a curvature change (singularity or near singularity depended on the change of surface topology [21]) which can induce two off-axis jets during the collapse of surface depression as indicated by the two arrows in Fig. 3. From the top view of the surface depression, this curvature change encircles around the thin jet and is called circular ring-shaped crater in the following discussions. It is the radially outward motion of the collapsing circular ring-shaped crater that results in the crown-like structure in Fig. 2, and this crown-like structure is well connected to the thick jet because of the same origin of the surface depression.

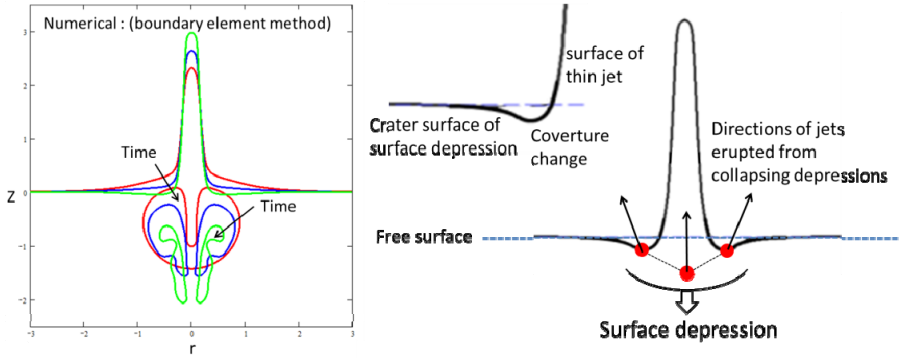

Fig. 3. The numerical simulation and curvature schematic of the surface depression are shown. The z and r of cylindrical coordinate are normalized to the R_{max} of the bubble.

Based on the requirement of the circular ring-shaped crater for the crown formation, the thin jet on the center of the surface depression is crucial for the crown formation. Because the thin jet is pushed by the bubble and the surface depression is caused from the downward decay of the bubble, the bubble depth should have a significance effect on the crown-like structure. To show this effect on the water jet from the free surface, Fig. 4 illustrates consecutive images as Fig. 2 but with three different γ-values. Based on distinctive morphologies of the crown, the γ-values are divided into four ranges, non-crown formation when $\gamma \leq 0.5$ (Fig. 4(a)), unstable crown formation when $0.5 \leq \gamma \leq 0.6$ (Fig. 4(b)), crown-like structure with complete crown wall when $0.6 \leq \gamma \leq 1.1$ (Fig. 2), and non-crown formation when $1.1 \leq \gamma$ (Fig. 4(c)).

#179203 - $15.00 USD Received 2 Nov 2012; revised 19 Dec 2012; accepted 19 Dec 2012; published 4 Jan 2013

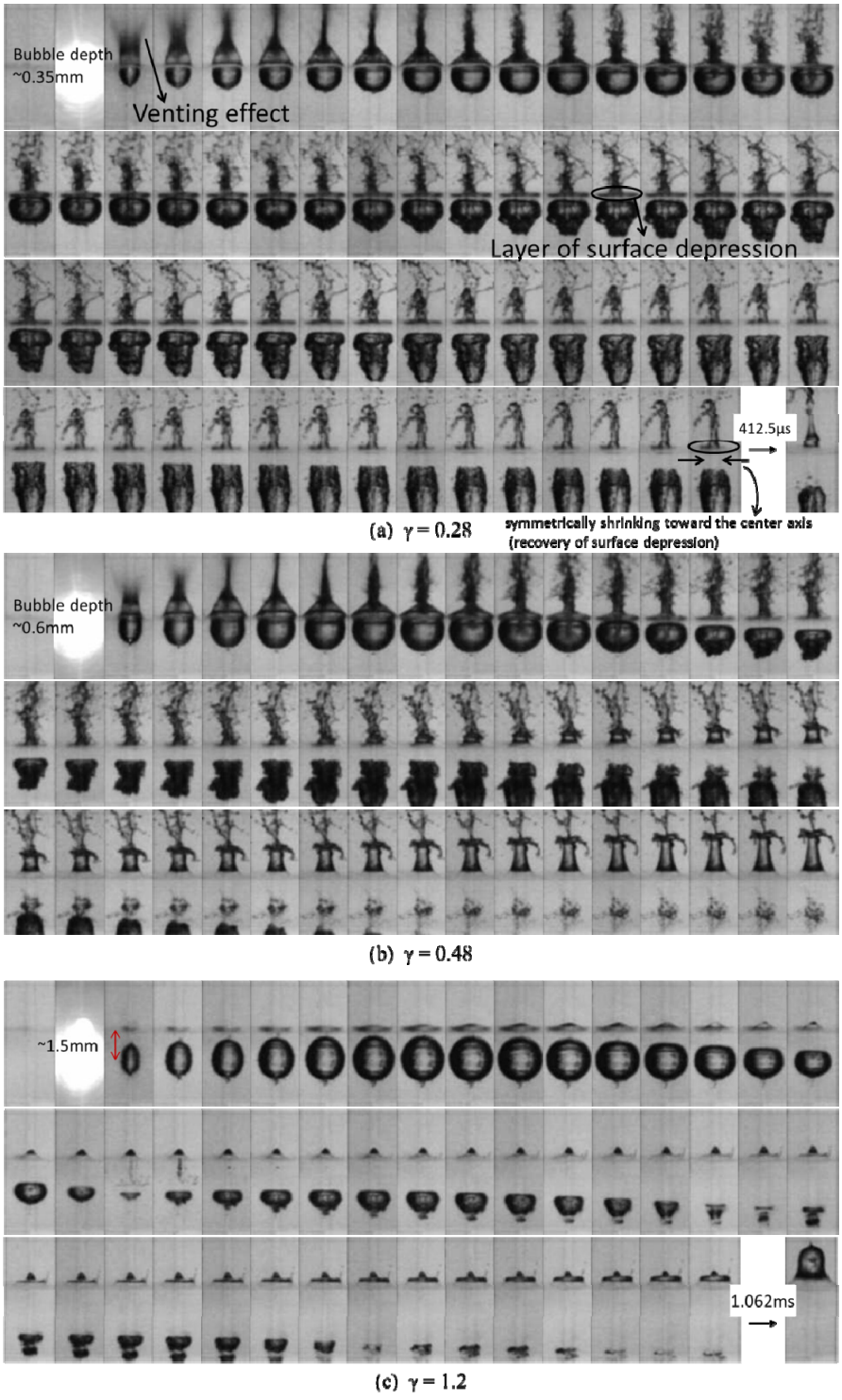

Fig. 4. The frame rate is 80,000 fps as same as Fig. 2. Figures 4(a) and (c) illustrate the non-crown formation when γ-value is smaller than 0.5 and larger than 1.1, respectively. Figure 4(b) shows another structure of the crown formation as compared to Fig. 2. This crown is denoted as unstable crown formation.

#179203 - $15.00 USD Received 2 Nov 2012; revised 19 Dec 2012; accepted 19 Dec 2012; published 4 Jan 2013

When the bubble is very near the free surface for $\gamma = 0.28$, as shown in Fig. 4(a), the surface depression can be clearly seen with a segment of black line (layer of surface depression) generated on the horizontal free surface after the sinking around the bottom of the thin jet. The black line symmetrically shrinks toward the center axis from its opposite ends, and finally a thick jet forms under the thin jet, as depicted in the last picture in Fig. 4(a). The slow depression and collapse of the surface sinking are due to the extremely slow collapse of the bubble. The strong interaction between the upper boundary of the bubble and the free surface during the first expansion phase leads to some energy loss from the bubble similar as a venting effect mentioned in Ref. 7. Such an evolution about this venting effect was described more detail in the studies of laser ablation on a surface [25,26]. This venting effect could explain the unusual slowdown of the collapse of the bubble. Besides the slow collapse, the upper boundary of the bubble is so close to the free surface that it obstructs the downward depression of the surface sinking. Thus, the depression of the surface is not strong enough for the crown-like formation despite the appearance of the thin and thick jets. When $\gamma = 0.48$, the venting effect is diminished and the strength of the surface depression is restored to a level as the case of $\gamma = 0.8$ (near velocity of the thick jet). However, the thin jet experiences a violent disruption when going through the breach of the free surface by the expansion of the bubble at an initial time. The scraggly surface on the thin jet will disrupt the circular ring-shaped crater, and the crown-like structure (or properly called a layer of water on top of the thick jet) is weak and unstable, as shown in Fig. 4(b). When $\gamma > 1.1$, the weak interaction between the free surface and the bubble leads to a diminished thin jet shaped like a small hill and weak surface depression. Such a surface depression is not large enough to cause the circular ring-shaped crater to reach the threshold of surface topology change [21] to induce the crown-like formation. However, the weak surface depression is still able to induce a slow thick jet with an approximate velocity of 1.4 m/s.

To see the evolution of bubble depth, Figs. 2 and 4 illustrate the morphologies of water jet for each γ-value of the above-mentioned four γ ranges. Detailed correlation between the thin jet and crown-like structure is shown in Fig. 5 with increasing γ from 0.5 to 1.02. For $\gamma = 0.5$, the morphologies show the splash of water from the breached surface into multiple droplets. It is difficult to distinguish the shape of the thin jet from the upward splash. This defective structure of the thin jet results in an unstable crown, similarly as shown in Fig. 4(b). Increasing γ can reduce the influence of the water splash on the thin jet which begins to show a continuous line structure, as implied in the fourth frame of Fig. 5 for $\gamma = 0.58$. The crown-like jet is still unstable, and thus the circular ring-shaped crater resulted from the surface depression should be still defective. When $\gamma \geq 0.6$, the splash is depressed and the crown structure becomes clear. When $\gamma = 0.7$, breached surface is absent and a pronounced growth of crown-like structure can be seen. The velocities of both the thin and thick jets decrease with increasing γ from 0.7 to 1.02 due to the depression of the surface interaction, and the height of the crown wall thus gradually decreases, and eventually disappears, as shown in Fig. 4(c). Figure 5 reveals that crown-like structure is always accompanied with a thin jet and becomes mature in structure when the thin jet is stabilized.

#179203 - $15.00 USD Received 2 Nov 2012; revised 19 Dec 2012; accepted 19 Dec 2012; published 4 Jan 2013

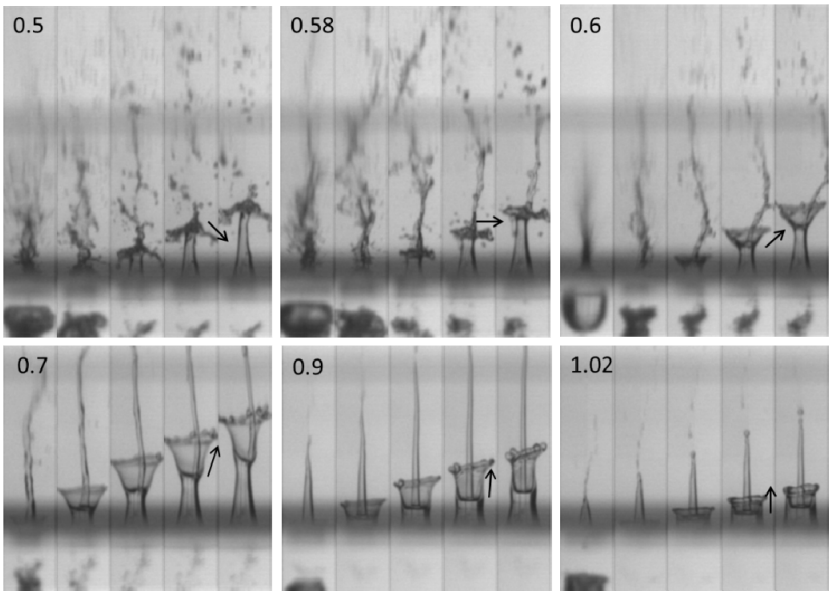

Fig. 5. The structures of the thin jets and crowns with different γ-values which are labeled on the left top of each image. The fame rate is 30,000 fps but the time interval between each frame is 0.166 ms. The arrow shows the orientation of the crown wall, which rotates counterclockwise to vertical direction when γ is increased from 0.5 to 1.02.

We have shown by Fig. 2 that the crown-like structure forms around the thick jet, which suggests a correlation between the crown formation and the origin of the thick jet. This correlation can be further confirmed by Fig. 5 in which, despite different orientations (defined by the arrows in Fig. 5) of the crown wall, the bottom of the crown-like structure always sits on the head of the thick jet. The orientation of the crown wall can be seen to gradually turn counterclockwise to vertical when γ is gradually increased from 0.5 to 1.02. The transition to a complete crown wall occurs when the arrow turns from downward (γ = 0.5) across the horizontal line (γ = 0.58) to upward (γ from 0.6 to 1.02). This feature shows a high regularity and correlation between the orientation of the crown wall and the depth of the bubble. For comparison, let us refer to Fig. 3 which shows the relation between the deformed surface depression (with the thin jet) and arrowed directions of the collapse of the circular ring-shaped crater. Based on Fig. 3, it is reasonable to infer that the directions of the circular ring-shaped crater should have a similar trend of rotation when the bubble depth is increased to change the surface depression. This comparability further suggests the crown-like formation is correlated to the surface depression with the thin jet (to induce the circular ring-shaped crater). From the continuous change of the orientation of the crown with increasing γ, the layer of water on top of the thick jet for $0.5 \le \gamma \le 0.6$ should be considered as a crown-like structure similar as that for $\gamma \ge 0.6$, and thus was denoted as "unstable crown formation" in the above discussions. Finally, as shown in Fig. 5, the top rim of the crown wall is nearly flat for $0.6 \le \gamma \le 1.02$, which is significantly different to the two-arm splash on the crown wall induced by spark discharge [7]. This difference is probably related to the unavoidable mechanical influence due to the electrodes in spark discharge. We believe that a laser is very suitable for studying the bubble-induced jet formation from a free surface, and these studies, if combined with a simple soft lithography technique, can be used to control the fluid flow in a microfluidic device, water-assisted laser processing or other applications of jet injectors.

#179203 - $15.00 USD Received 2 Nov 2012; revised 19 Dec 2012; accepted 19 Dec 2012; published 4 Jan 2013

4. Conclusion

We have studied the morphologies of the water jet generated from the laser-induced bubble under the flat water surface. The crown formation is caused by the collapse of a circular ring-shaped crater which is due to a thin jet on the center of the surface depression. The evolution of the bubble depth shows that the crown-like structure is always accompanied with the thin jet and becomes mature in structure when the thin jet is stabilized. Measured results revealed a correlation between the orientation of the crown wall and the bubble depth. This correlation is explained by the directional change of the collapse motion of the circular ring-shaped crater.

Acknowledgments

The authors also thank the National Science Council for their financial support of this research under Contract No. NSC-97-2112-M-009-016-MY3.

#179203 - $15.00 USD Received 2 Nov 2012; revised 19 Dec 2012; accepted 19 Dec 2012; published 4 Jan 2013